Cellulose (2017) 24:4383–4392
DOI 10.1007/s10570-017-1416-5

ORIGINAL PAPER

Chitosan-based polymer gel paper actuators coated with multi-wall carbon nanotubes and MnO_2 composite electrode

Zhuangzhi Sun · Wenlong Song · Gang Zhao · Haojun Wang

Received: 22 June 2017 / Accepted: 15 July 2017 / Published online: 27 July 2017

Abstract In this work, MCNT/MnO_2 composite electrode actuators were fabricated by ultrasonic oscillating adsorption of MnO_2 on both sides of the MCNT coated chitosan membrane. Elemental composition determined by an energy-dispersive spectrometer showed that the doping MnO_2 was successfully adsorbed on the surface of MCNT. Surface morphologies of actuators under different doping MnO_2 ratios (0, 0.1, 0.25, 0.5, 1) were characterized using scanning electron microscopy. The electromechanical properties of actuators were further given by the experimental test platform, and the electrochemical properties of actuators were analyzed using cyclic voltammetry (CV). CV results revealed that the changing trends of specific capacitance and output force density, specific capacitance and strain were basically the same. When the ratio of MnO_2 was less than 0.5, the former performance increased rapidly, while higher than 0.5, the latter grew faster. The experimental results showed that the adsorption content of MnO_2 particles was affected by changing the conductivity of the electrode layer, which affected the electromechanical properties of actuators.

Keywords Polymer gel · Electrochemical properties · Ultrasonic adsorption · Specific surface area

Z. Sun (✉) · W. Song
Province Key Laboratory of Forestry Intelligent Equipment Engineering, School of Mechanical and Electrical Engineering, Northeast Forestry University, Harbin 150000, People's Republic of China
e-mail: sunzhuangzhi@nefu.edu.cn

Z. Sun · W. Song
Ministry of Education Key Laboratory of Bio-based Material Science and Technology, Northeast Forestry University, Harbin 150000, People's Republic of China

G. Zhao · H. Wang
School of Mechanical and Electrical Engineering, Harbin Engineering University, Harbin 150000, People's Republic of China

Introduction

Ionic polymer gel paper, which is classified with ionic electro-active polymers (EAPs), exhibits bending deformation when a small electrical potential is utilized on its surface (Kumar et al. 2016; Ishii et al. 2017; Uh et al. 2016; Shintake et al. 2016). The fascinating characteristics of polymer gel paper including softness, lightweight, biocompatibility, flexibility and large displacement have achieved concentrated interest for a wide range of intelligent agents and automation as soft actuators (Shoji 2016; Gu et al. 2015; Sait and Muthuswamy 2016; Shintake et al. 2016). As a kind of EAPs, ionic polymer gel paper is typically composed of a thin cation-exchange polymer, which allows multiple charges to pass, and a pair

of electrodes, which are fabricated by the hot-pressing technique. The most interesting property of EAPs is its flexibility, which can be utilized as a potential candidate for the flexible fabrication in products, and it can also be applied to fabricate miniature manufacturing systems and biological equipment in the practical engineering area (Xu et al. 2015; Lee et al. 2013). Furthermore, the fabrication process of EAPs, especially for MEMS areas, requires a simple and environmentally friendly process and a low-energy cost instead of traditional processes using toxic gases (Sait and Muthuswamy 2016; French 2014; French et al. 2014; Nam et al. 2016).

It has been confirmed that the actuation performance of ionic EAPs is mainly dominated by the electrochemical and electromechanical process of the electrode layer (Kim et al. 2014; Hadden et al. 2014). Thus, the electrode material and the electrode structure become more crucial to achieve bending paper with excellent performance. Also, the electrode materials with higher conductivity, well flexibility and appropriate electrochemical and electromechanical properties are of great importance for various application areas. Recently, carbon nanotubes (CNT) and carbon black (CB) with high surface area, exceptional conductibility, chemical characteristics, and electromechemical double-layer capacitors have been widely introduced into the electrode membrane (Rogers and Liu 2011; Li et al. 2004; Terasawa and Asaka 2016). They also behave with some significant improvement including quick response speed, large bending deflection and strain rate, etc. However, carbon nano-structures have low capacitance, which still can be improved by compositing with other materials.

MnO_2, regarded as an excellent electrode material, is widely used in super capacitors as good energy storage material. As a kind of semiconductor, due to its large specific surface area and high electrochemical properties, MnO_2 has various properties of nanomaterials. Its microstructure is different according to different preparation conditions. According to the different crystal form, MnO_2 can be divided into three categories; the first category of the one-dimensional tunnel structure, the second category of the two-dimensional layered structure, and the third category of interconnected three-dimensional channel structure. MnO_2 has the advantages of wide preparation of raw materials, low price, reducing environmental pollution. Hence, the high conductivity, chemical stability and high specific capacitance of MnO_2 were combined with multi-walled carbon nanotubes (MCNT), which were mixed with its aqueous dispersion by the ultrasonic cell pulverizer. MnO_2 particles were adsorbed with MCNT in order to achieve the purpose of improving its specific capacitance.

Hence, it is necessary to investigate the effects of various doping contents of semiconductor MnO_2/MCNT. Therefore, the purpose of this manuscript is to investigate a bio-inspired chitosan-based polymer gel paper with a semiconductor MnO_2/MCNT composite electrode. Through the electrochemical properties research of chitosan-based polymer gel paper, the relationship between the electromechanical properties and the electrochemical properties was further figured out.

Material and method

Chitosan powder (deacetylation degree 85.66%, viscosity 450 mPa s, CS powder) was purchased from HaiDebei Marine Bioengineering Company (Jinan, China). Multi-walled Carbon Nanotube Dispersion (MCNT, deionized water solvent, 70 wt‰ carbon nanotube content), glycerol, acetic acid, deionized water, were applied as the ingredients.

Preparation processes of polymer gel paper include the following three steps, electrolyte layer, electrode

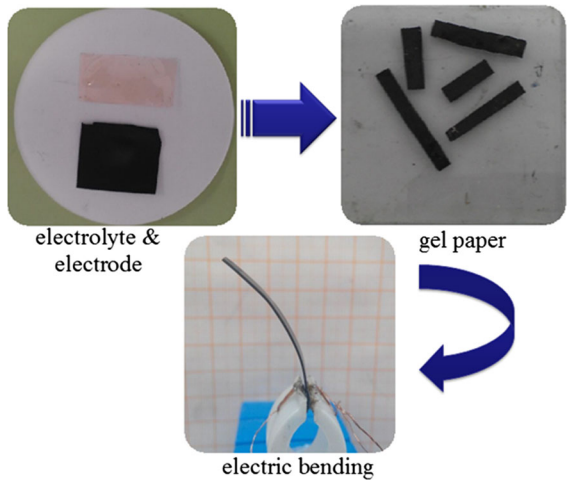

Fig. 1 Schematic structure of polymer strip composed of a chitosan polymer supported electrolyte layer sandwiched by MCNT electrode layers

layer, and manufacturing assembly, as shown in Fig. 1. The specific process preparation process is as follows.

1. Preparation of electrolyte layer. The temperature of the magnetic stirrer was set at 60 °C, and the heating time was 30 min. A range of a 250 mL beaker containing 50 mL water was placed in the middle of that stirrer. Then, 15 mL 2% (volume fraction) acetic acid solution was measured into a 50 mL standard beaker. In addition, 0.3 g chitosan was weighed on the analytical balance, and the stirrer was gradually added to the appropriate stirring speed for 15 min. Then, the mixed solution was placed in an ultrasonic cleaner and was subjected to the defoaming treatment to remove the bubble for 30 min. All the solution was set in a glass mold, with size 50 mm × 50 mm and with a wait until it flowed evenly. The temperature of the vacuum oven was set at 80 °C, and the drying time was 4 h. Also, the vacuum degree was zero, and the platform was adjusted by a gradienter. Finally, it was cooled down in the vacuum oven slowly to obtain an electrolyte membrane of an actuator.
2. Preparation of electrode layer. MCNT aqueous solution was secondarily broken up by ultrasonic cell pulverizer under the conditions of the working time of 5 min, the ultrasonic time of 1.5 s after 2 s break, and the protection temperature 60 °C. It meant during the ultrasonic shock process, the ultrasonic oscillation worked 1.5 s after a 2 s break. During this work cycle, ultrasonic equipment shocked about 5 min before stopping. Then, 5 mL 2% acetic acid and 0.06 g of chitosan were mixed in a water bath beaker, and then they were stirred for 15 min by moderate speed. After dissolving, 2.5 mL dispersed MCNT aqueous dispersions were transferred into a beaker and stirred for another 15 min. Then, 20 mL MCNT aqueous dispersions 10% (mass fraction) was placed in a 200 mL beaker and 80 mL distilled water was added to 2% (mass fraction) dilute. Also, 0.2 g of MnO_2 was weighed into the beaker and placed in an ultrasonic cell disperser. When the mixed solution broke up several times, the temperature exceeded the protection temperature 60 °C. After taking it out until being cooled down, MnO_2/MCNT doping ratio of 0.1 mixed solution was prepared. A mixed solution of MnO_2/MCNT doping ratio of 0.25, 0.5, 1 was prepared by ultrasonic adsorption under the same processes. In addition, a 10 mL mixed solution was added to the mixture and was proceeded by the defoaming treatment for 15 min. Then, it was poured it into a glass mold sized 50 mm × 50 mm evenly. With the experimental conditions of the drying temperature 80 °C, the drying time 6 h, the vacuum degree zero, electrode membranes with MnO_2/MCNT doping ratios of 0.1, 0.25, 0.5 and 1 were prepared, respectively. In this part, the quality ratio was regarded as the measurement unit of MnO_2/MCNT.
3. Manufacturing assembly. The electrode membrane and the electrolyte membrane were cut into a size of 3.5 mm × 5 mm. The two electrode membranes and the electrolyte membrane were placed on clean filter paper. The hot-pressing temperature was set at 30 °C and the hot-pressing pressure was 0 MPa. Depending on the pressure of hot-pressing for 20 min, a bio-inspired chitosan-based polymer gel paper was obtained. The samples were tested under the direct current (DC) excitation, and the result is shown in Fig. 1. Under DC excitation, our polymer paper produced a bending deflection in the direction of the cathode.

Figure 2 displays a schematic diagram of the experimental setup for polymer gel paper. A signal generator (SP1651 typed digital synthesis of the low-

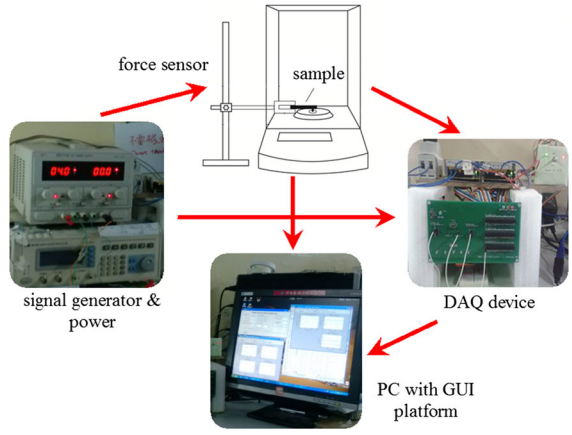

Fig. 2 A schematic diagram of the experimental setup for polymer gel paper

frequency signal generators) is utilized to activate polymer paper. The conditioning circuit and the data-acquisition card are integrated in a DAQ device. The PC is implemented to control and communicate between a DAQ device and the software operation platform established by a GUI module in Matlab 2012a. A high-speed frequency camera is used for collecting transient movement from polymer gel paper. A current sensor is applied to acquire the feedback current signal of the experiment. Finally, the data is processed directly by using Matlab 2012a. In this experiment, the electrochemical properties of polymer gel paper are mainly measured as follows. The double-layer capacitance of the polymer-supported electrode is calculated by cyclic voltammetry (CV) using a multi-channel chemical test station (Vmp3). The morphology is characterized by a scanning electron microscope (SEM, JEOL JSM-6480). All measurement data presented here are an average of five samples.

Results and discussion

In order to show that the ultrasonic oscillating process can realize the adsorption of MnO_2 particles on the MCNT, the electrode membrane with MnO_2 doping ratio of 0.5 was scanned to detect the element contents of Mn, O and C. EDS tests were performed at two random locations of the same experimental sample, as shown in Fig. 3.

Table 1 is the mass percentage and atomic number at different locations of the electrode membrane. It shows that both positions can observe the elements of Mn and O. The mass percentages of Mn were 5.92 and 5.91%, respectively, and the atom percentages were both 1.42%. The mass percentages of O elements were 14.05 and 13.06%, and the atom percentages were 11.61 and 10.17%, respectively. According to the elemental composition of polymer gel material, MnO_2 was successfully doped on the electrode layer to a certain extent, and it was also indicated that the ultrasonic wave can adsorb MnO_2 on the surface of MCNT. In order to observe the dopant MnO_2 on the MCNT clearly, the adsorbed MnO_2 particles were scanned by high multiplier SEM for further explanation.

The surface morphology of the electrode membranes with different MnO_2 doping ratios were analyzed by SEM with the field emission. Figure 4 shows the microstructure of the electrode membranes with different MnO_2 doping ratios at magnifications of 20,000 times and 50,000 times. It was obvious that there was a large difference in the microstructure of the electrode membranes with different MnO_2 ratios. The results of the energy spectrum analysis showed that the small particles of MnO_2 had adsorbed on the surface of MCNT. Combining with the electrode surfaces in the magnifications of 20,000 times and 50,000 times, the conclusion is summarized as follow. When MnO_2 doping ratio was 0, there was no MnO_2 particle on the MCNT. When the MnO_2 doping ratio was between 0.1 and 0.25, a small amount of MnO_2 particles were adsorbed on the MCNT. When the MnO_2 doping ratio was 1, the number of MnO_2 particles adsorbed on the MCNT did not show a significant increasie. This indicated that MCNT had formed by an ordered network structure, and the adsorption force of MnO_2 particles was limited when forming the network structure. As the content of adsorbed MnO_2 particles exceeded 1, the adsorption capacity of MCNT was almost saturation, and MnO_2 particles could not be adsorbed by MCNT.

The output force of polymer gel paper with different doping ratios of MnO_2 was measured by experimental test platform. The variation characteristics of 150 s time and 300 data points were tested. The data points were fitted with a polynomial by Origin 9.1, and the polynomial fitting graph of polymer gel paper with different MnO_2 doping ratios was obtained, as shown in Fig. 5a. The first 40 s of the output force with time were tested, and the data points were used for straight line fitting. The linear slope was approximately the response rate of the output polymer gel paper. The maximum output force and response rates are shown in Fig. 5b. The fitting curves of the output strain of polymer gel paper at a different time were obtained by measuring the output displacement including 300 data points and 90 s using the conversion of strain formula. The output force density (mN/s) is defined as the maximum output force that can be provided by unit mass, and the formula is $S = F/m$, where F represents the maximum output force (mN) of polymer gel paper, and m is the mass of polymer gel paper. The curves of output density and strain for the different doping ratios are shown in Fig. 6.

By analyzing the variation trend in Fig. 5a, it could increase the output force of polymer gel paper by doping MnO_2 in the electrode membrane. With the

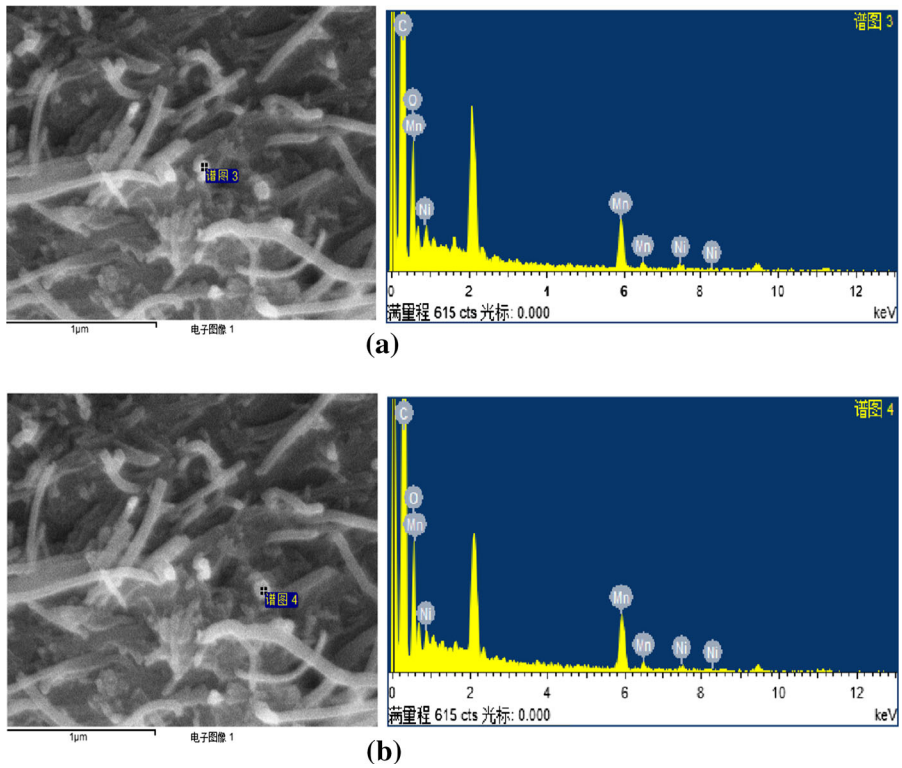

Fig. 3 EDS microsatellite scanning of the electrode membrane doped with MnO_2 ratio of 0.5: **a** position 1, **b** position 2

Table 1 Element contents in the electrode membrane doped with MnO_2 ratio of 0.5

Element	Position 1		Position 2	
	Mass (%)	Atomicity (%)	Mass (%)	Atomicity (%)
C	78.76	86.68	79.74	87.53
O	14.05	11.61	13.06	10.17
Mn	5.92	1.42	5.91	1.42

increase of MnO_2 doping ratio, the output force of polymer gel paper changed smoothly, and there was no obvious volatility. In order to analyze the performance effect of polymer gel paper with different MnO_2 doping ratios intuitively, the variations of the output force and response speed of the polymer gel paper were plotted by Origin 9.1, as shown in Fig. 5b. The output force of polymer gel paper declined after rising with the increase of MnO_2 doping ratio. When the ratio of MnO_2 doping reached 0.5, the output force of polymer gel paper was the largest of 3.3 mN. The variations of output force density and strain are shown in Fig. 5b. The response rate of the polymer gel paper increased with the increasing of the MnO_2 doping ratio. However, when the MnO_2 doping ratio was more than 0.5, the response rate increased significantly after a slowdown. When MnO_2 doping ratio reached 1, the response rate reached the maximum of 0.05 mN/s.

Figure 6 shows the output force curves of polymer gel paper with different MnO_2 doping ratios. It can be seen that the output force density and strain of the polymer gel paper increased with the increase of MnO_2 doping ratio. When the MnO_2 doping ratio did not reach 0.5, the increasing trend of the output force density and strain were larger. When the MnO_2 doping ratio exceeded 0.5, the increasing trend of the output force density and strain of polymer gel paper became slower. This is due to the increase doping of MnO_2 particles adsorbed to MCNT by ultrasonic shock increase. However, when MnO_2 particles doping increased to a certain amount, the particles adsorbed on the MCNT would reach saturation, which meant

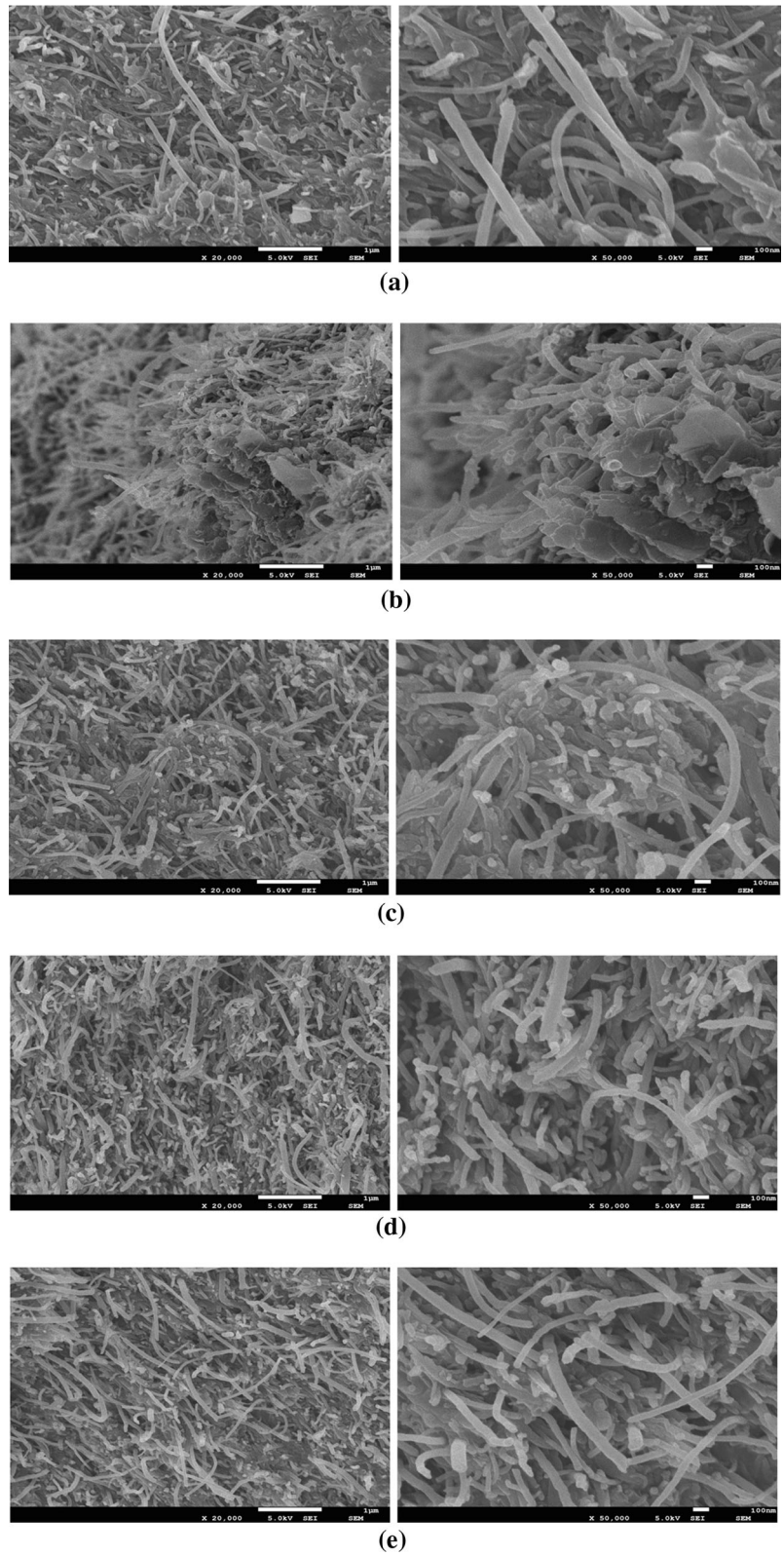

Fig. 4 Microscopic morphology in the doping of different MnO_2 ratios of the electrode membrane in the amplification of 20,000 times (*Left*) and 50,000 times (*Right*). **a** 0, **b**, 0.1, **c** 0.25, **d** 0.5, **e** 1

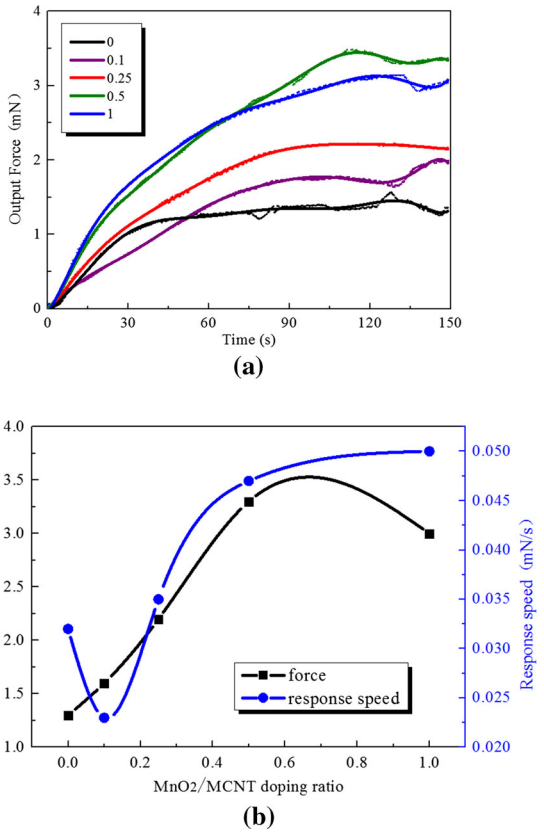

Fig. 5 **a** Comparison of output force changing with time, **b** the output force and response speed with different doping ratio of MnO_2

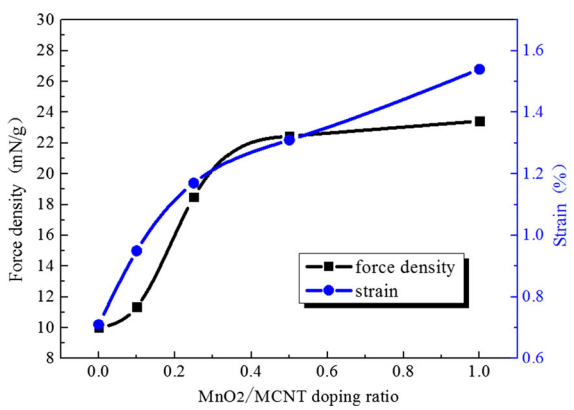

Fig. 6 The change of output force density and strain with MnO_2 doping ratio

even if the MnO_2 content was increased, the doping effect would not be changed. When the ratio of MnO_2 doped in the electrode membrane reached 0.5, the polymer gel paper had excellent output performance. In particular, the output force density was 22.45 mN/g, and the strain was 1.31%. Comparing with the output performance of unoptimized polymer gel paper, it increased by 125 and 85%, respectively.

The above studies proved that the mechanical properties of MCNT with MnO_2 particles were significantly improved. As an excellent energy storage semiconductor material, MnO_2 owns a large surface area and a high electrochemical performance, and it is also equipped with properties of nano-materials. The microstructure is different depending on the preparation conditions. In order to analyze the improvement of the electromechanical properties by doping MnO_2 in an electrode membrane, the current–voltage (CV) characteristics curves of the electrode membranes doped with MnO_2 ratios of 0, 0.1, 0.25, 0.5, 1 were measured to research. The effect of doped MnO_2 particles on the specific capacitance of the electrode membrane was experimented with at the sweep speed of 100 mV/s.

Figure 7 showed a typical charge and discharge characteristic of the electric double layer in electrochemistry, because CV characteristics of the electrode membrane tended to be rectangular. By calculating the area surrounded using the current–voltage characteristic of the electrode membrane doped with the MnO_2 ratio of 0, 0.1, 0.25, 0.5, the specific capacitance was 0.92, 0.93, 1.41, 2.35, 2.5 9 F/g, respectively. It can be seen that the addition of MnO_2 in the electrode membrane could improve the specific capacitance. In order to clearly obtain the effect of MnO_2 doping ratio on the specific capacitance, the change ratio of the

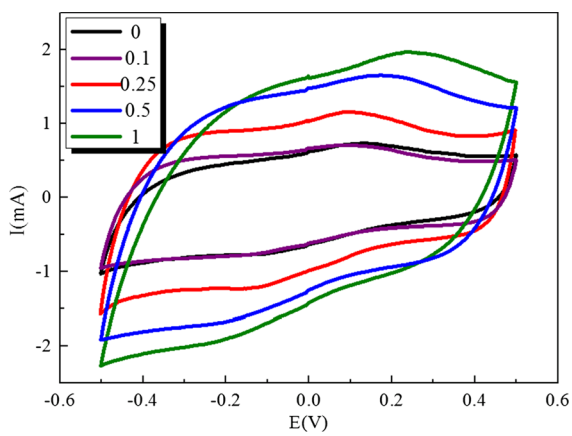

Fig. 7 CV curves with different MnO_2 doping ratios at 100 mV/s sweep speed

MnO_2 doping ratio was plotted and the data points had polynomial fitting for four times, as shown in Fig. 8. It was found that the specific capacitance of the electrode membrane increased with the increase of the ratio of MnO_2. When the ratio of MnO_2 doped was between 0.1 and 0.5, the specific capacitance of the electrode membrane increased linearly rapidly. When the ratio of MnO_2 doped was more than 0.5, the specific capacitance had little increase. When the ratio of MnO_2 doped was just in 0.5, the specific capacitance of the electrode membrane was increased from 0.92 to 2.35 F/g, which was 1.6 times higher than that of undoped MnO_2. The capacitance of the electrode surface accommodating the electron content mainly depended on the specific surface area of the electrode surface layer. Although the surface area of the MCNT electrode increased, the number of electrons adsorbed on the surface of the MCNT electrode was limited. As a result, the specific capacitance of the electrode surface layer did not increase.

In order to further study the effect of the electrochemical characteristics on the electromechanical properties, the variations between the output force density and specific capacitance, strain and specific capacitance were analyzed under different MnO_2 doping ratios.

By the analysis of Fig. 9a, the specific capacitance and the output force density of the electrode membrane increased with the increase of the MnO_2 doping ratio, and the growth trend was nearly the same. When the ratio of MnO_2 doped in the electrode membrane was between 0.1 and 0.5, the specific capacitance of the electrode membrane and the output force density of the polymer gel paper were increased rapidly. When the ratio of MnO_2 doped in the electrode membrane was more than 0.5, the specific capacitance of the electrode membrane and the output force density of the polymer gel paper increased extremely slowly. Through the analysis of Fig. 9b, with the increase of MnO_2 doping ratio, the specific capacitance of the electrode membrane and strain of the polymer gel paper increased, and the increase trends were also similar. When the ratio of MnO_2 doped in the electrode membrane was 0.1–0.5, the specific capacitance and the strain were increased rapidly. When the ratio was 0.5, the strain still had a good improvement. When the ratio over 0.5, the increase of specific capacitance nearly stopped, and the strain still increased slowly.

As previously discussed, the electrode layer doped with MnO_2 particles can increase the specific surface

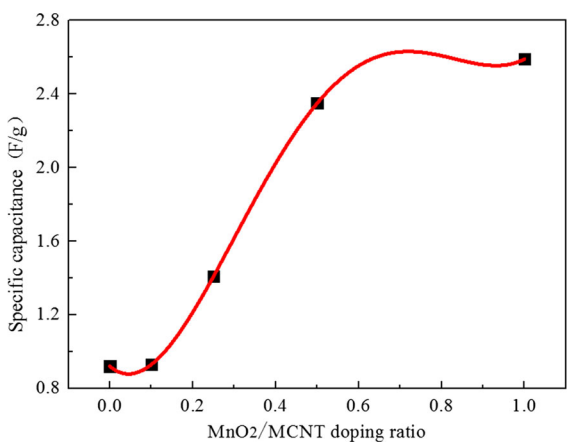

Fig. 8 Comparison of the specific capacitance of the electrode membrane with MnO_2 doping ratio increase

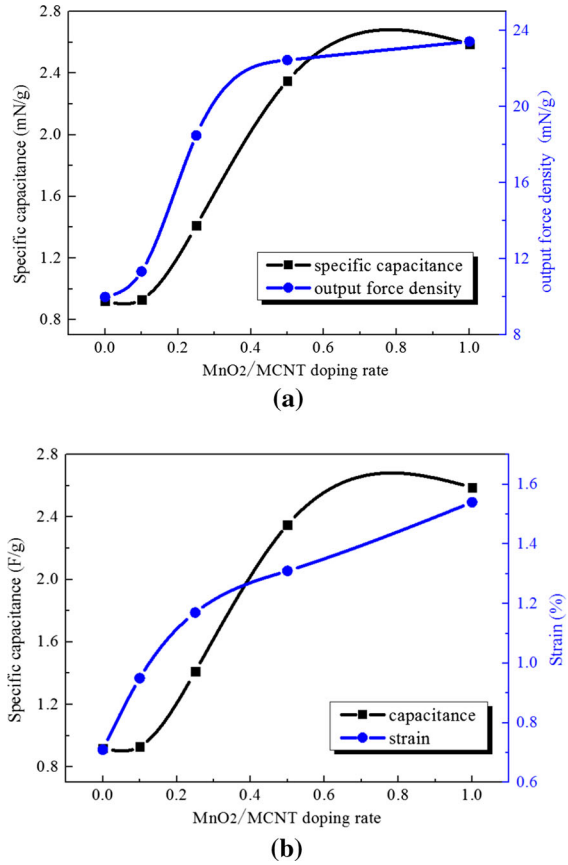

Fig. 9 Effect of specific capacitance of the electrode membrane on MnO_2 doping ratio: **a** output force density, **b** strain

area of MCNT. This increased the specific capacitance of the electrode layer and enhanced the ability of the electrode membrane to accommodate electrons. After applying DC voltage at both bottoms of polymer gel paper to stimulate more electrons in the interface layer, a high electric field at both ends of the electrolyte membrane was formed. The migration rate and volume of ions in the electrolyte membrane were improved. As the increase of the cumulative amount of ion transporting to bonding surface in the electrolyte layer increased, the output force of polymer gel paper increased, and the output force density of polymer gel paper was enhanced.

The increasing of the output force could significantly improve the bending deformation capacity of the polymer gel paper, thereby the strain of polymer gel paper was improved. In addition, when the MnO_2 doping ratio exceeded 0.5, the MnO_2 particles adsorbed on the MCNT were nearly saturation. Under this condition, MnO_2 particles could not be adsorbed on the MCNT anymore. When the MnO_2 doping ratio exceeded 0.5, the specific capacitance of the electrode membrane grew slowly, and the output force density of polymer gel paper increased slowly.

Conclusions

In summary, in this manuscript, a bio-inspired chitosan-based polymer gel paper with various doping contents of semiconductor MnO_2/MCNT composite electrode were fabricated by ultrasonic adsorption. When electrode films doped with MnO_2 at 0.5%, the atomic percentages of Mn elements at different positions were 5.92 and 5.91%, respectively, which indicated that the ultrasonic oscillating process could adsorb MnO_2 on MCNT. The microstructures of the electrode films with different MnO_2 doping ratios were analyzed by scanning electron microscopy (SEM).

The results showed that the number of MnO_2 particles adsorbed network-like structure generated by MCNT was limited. Therefore, when the MnO_2 doping ratio was 1, the adsorption amount of MnO_2 particles did not increase. When the doped ratio of MnO_2 in the electrode film was 0.5, the actuator had excellent output electromechanical properties. The output force density was 22.45 mN/g and strain was 1.31%. Compared with the unoptimized actuators, the output force density and the strain were increased by 125 and 85%. When the MnO_2 doping ratio was 0.5, the output force of the actuator was the largest at 3.3 mN, while the MnO_2 doping ratio was 1, the response rate reached the maximum of 0.05 mN/s. When the ratio of MnO_2 doped was 0.5, the specific capacitance of the electrode film was increased from 0.92 to 2.35 F/g, which was 1.6 times higher than that of undoped MnO_2.

When the ratio of MnO_2 was less than 0.5, performance of specific capacitance and output force density increased rapidly. While higher than 0.5, performance of specific capacitance and strain grew faster. Because the electrode layer doped with MnO_2 particles is improved by increasing the specific surface area of MCNT, thereby the specific capacitance of the electrode layer is increased. Also, the ability of the electrode film to accommodate electrons is enhanced, and the output force density of actuators is improved. However, when the MnO_2 doping ratio exceeds 0.5, the adsorption of MnO_2 particles in the MCNT is close to saturation. The specific capacitance of the electrode film is slow to increase, and the output force density of actuators also increases slowly.

Acknowledgments We gratefully acknowledge the financial support from the National Science Foundation of China (No. 31470714) and the Fundamental Research Funds for the Central Universities (No. 2572017BB08).

References

French AD (2014) Idealized powder diffraction patterns for cellulose polymorphs. Cellulose 21(2):885–896

French AD, Concha M, Dowd MK et al (2014) Electron (charge) density studies of cellulose models. Cellulose 21(2): 1051–1063

Gu YQ, Mou JG, Dai DS (2015) Characteristics on drag reduction of bionic jet surface based on earthworm's back orifice jet. Acta Phys Sin Chin Ed 64(2):024701

Hadden JA, French AD, Woods RJ (2014) Effect of microfibril twisting on theoretical powder diffraction patterns of cellulose Iβ. Cellulose 21(2):879–884

Ishii S, Kokubo H, Hashimoto K (2017) Tetra-PEG network containing ionic liquid synthesized via michael addition reaction and its application to polymer actuator. Macromolecules 50(7):2906–2915

Kim J, Jeon JH, Kim HJ (2014) Durable and water-floatable ionic polymer actuator with hydrophobic and asymmetrically laser-scribed reduced graphene oxide paper electrodes. ACS Nano 8(3):2986–2997

Kumar K, Knie C, Bléger D (2016) A chaotic self-oscillating sunlight-driven polymer actuator. Nat Commun 7:11975

Lee SW, Kim JW, Kim YH (2013) Actuation characteristics of all-organic polymer actuator with conducting polymer electrode. Macromol Res 21(6):699–703

Li C, Wang D, Liang T (2004) A study of activated carbon nanotubes as double-layer capacitors electrode materials. Mater Lett 58(29):3774–3777

Nam S, French AD, Condon BD (2016) Segal crystallinity index revisited by the simulation of X-ray diffraction patterns of cotton cellulose Iβ and cellulose II. Carbohyd Polym 135:1–9

Rogers GW, Liu JZ (2011) High-performance graphene oxide electromechanical actuators. J Am Chem Soc 134(2): 1250–1255

Sait U, Muthuswamy S (2016) A study on the effect of surface topography on the actuation performance of stacked-rolled dielectric electro active polymer actuator. Funct Mater Lett 9(03):1650042

Shintake J, Rosset S, Schubert B (2016) Versatile soft grippers with intrinsic electroadhesion based on multifunctional polymer actuators. Adv Mater 28(2):231–238

Shoji E (2016) Fabrication of a diaphragm micropump system utilizing the ionomer-based polymer actuator. Sensor Actuat B Chem 237:660–665

Terasawa N, Asaka K (2016) High-performance PEDOT: PSS/single-walled carbon nanotube/ionic liquid actuators combining electrostatic double-layer and faradaic capacitors. Langmuir 32(28):7210–7218

Uh K, Yoon B, Lee CW (2016) An electrolyte-free conducting polymer actuator that displays electrothermal bending and flapping wing motions under a magnetic field. ACS Appl Mater Interfaces 8(2):1289–1296

Xu X, Zhou J, Nagaraju DH (2015) Flexible, highly graphitized carbon aerogels based on bacterial cellulose/lignin: catalyst-free synthesis and its application in energy storage devices. Adv Funct Mater 25(21):3193–3202